Appl Biochem Biotechnol (2015) 176:2290–2302
DOI 10.1007/s12010-015-1718-8

Bioprocess Evaluation of Water Soaking-Based Microbiological Biodegradation with Exposure of Cellulosic Microfibers Relevant to Bioconversion Efficiency

Jin Seop Bak[1,2]

Received: 1 May 2015 / Accepted: 15 June 2015 /
Published online: 28 June 2015

Abstract To verify the interconnective relationship between biodegradation efficiency and microfibril structure, recalcitrant rice straw (RS) was depolymerized using water soaking-based microbiological biodegradation (WSMB). This eco-friendly biosystem, which does not predominantly generate inhibitory metabolites, could increase both the hydrolytic accessibility and fermentation efficiency of RS. In detail, when swollen RS (with Fenton cascades) was simultaneously bio-treated with *Phanerochaete chrysosporium* for 12 days, the biodegradability was 65.0 % of the theoretical maximum at the stationary phase. This value was significantly higher than the 30.3 % measured from untreated RS. Similarly, the WSMB platform had an effect on the yield enhancement of ethanol productivity of 32.5 %. However, uniform exposure of fibril polymers appeared to have little impact on bioconversion yields. Additionally, the proteomic pools of the WSMB system were analyzed to understand either substrate-specific or nonspecific biocascades based on the change in microcomposite materials. Remarkably, regardless of modified microfibril chains, the significant pattern of 14 major proteins (|fold| > 2) was reasonably analogous in both systems, especially for lignocellulolysis-related targets.

Keywords Bioethanol · Cellulose microfibril · Fungal proteome · Lignin · Water soaking-based microbiological biodegradation

Electronic supplementary material The online version of this article (doi:10.1007/s12010-015-1718-8) contains supplementary material, which is available to authorized users.

✉ Jin Seop Bak
jsbwvav7@kaist.ac.kr

[1] Department of Chemical and Biomolecular Engineering, KAIST, 291 Daehak-ro, Yuseong-gu, Daejeon 305-701, Republic of Korea

[2] Department of Chemical Engineering, MIT, 77 Massachusetts Avenue, Cambridge, MA 02139, USA

Introduction

The use of carbon-based green biofuels from renewable cellulosic biomass is being encouraged as an ideal concept for alternative energy, owing to the exhaustion of conventional fossil-based fuels in addition to undesired environmental consequences, especially global warming. First, to widely generalize the conventional ethanol bioprocess, an effective deconstruction process, based on the enzymatic inaccessibility from noncrystalline structures of cross-linked plant cell walls, is essential for the metabolic, biocascading conversion of recalcitrant polymeric chains into biodegradable fragments [1, 2].

Recent reports of biomass depolymerization have focused on structural modification methodologies, especially delignification, using large-scale, conventional systems, especially ammonia-soaking and dilute acid pretreatments, to enhance the industrial hydrolysis yields in a more cost/time-efficient manner [3, 4]. In reality, the severe dose of the conventional platforms may contribute to the direct enrichment of the theoretical maximum potential, as it is over 70 % of the bioconversion efficiency without considering inhibitory byproducts (especially furfurals) [5]. However, based on the one-sided disruption of primary barriers, particularly recalcitrant lignins, these platforms cannot be utilized for practical applications such as the effective verification of cellulolytic or hemicellulolytic enzymatic cascades, to conserve the yield of bioprocesses. In particular, the structural conversion ratio (i.e., crystallinity index [CrI]) of either amorphous or crystalline polymeric structures is critical when determining the binding type and efficiency of either oxidative or hydrolytic enzymes [6, 7]. Nevertheless, based on the integrated platform of conventional pretreatment processes, proactive modifications, such as exposure, aggregation, and loss of components, of cellulosic microfibrils to enhance the biomass digestibility have not been sufficient to form a generally accepted conceptual framework. More importantly, based on current technology, it is difficult for useful pretreatments to induce or extract the microfibril aggregates without causing environmental damage, owing to the inevitable necessity for chemical materials.

In this study, to address the indirect interrelationship between open microfibril aggregates and specific bioprocessing indices, especially enzymatic digestibility, crystallinity, and fermentability, the water-soaking platform for pretreating lignocellulosic substrates was used as part of an eco-friendly microbiology-based biodegradation system. In particular, process optimization was used to identify the important synergistic targets of enzymatic hydrolysis. Furthermore, to systematically understand the major lignocellulolytic cascades of the water soaking-based microbiological biodegradation (WSMB) program, the changing pattern of proteomic profiles was evaluated using a mass spectrometry-based approach at the "omics" level. Its impact was based on the economic feasibility and cultural stability of the WSMB biosystem upon exposing cellulosic microfibers. Lastly, an advanced understanding of the substrate-specific mechanism, based on open microfibrils via structural modification, is provided to manage the biodegradation processes or yields of this fungus and thus to better identify its substrates.

Materials and Methods

WSMB System

Air-dried lignocellulosic rice straw (RS) was used as a biomass model compound for the WSMB process. The dried RS was milled using an MF 10 milling machine (IKA, Staufen, Germany). The milled RS in the size range of 425–710 μm was dried in a vacuum-drying oven at 45 °C, and RS

contained more than 97.0 % (*w*/*w*) solid content. Prior to the biodegradation, RS was soaked in mineral water (containing 0.01 g/L $FeSO_4$; [8]) for 2 h at 25 °C to enhance the effect of substrate depolymerization (especially by the Fenton reaction). The degree of moisture content (based on solid/liquid ratios; *w*/*v*) used was 0 % (0; control) and over 81 % (0.25; colloidal suspension). To prevent the loss of moisture from pretreated RS, all samples were instantly packed in a polystyrene bag under vacuum after soaking until WSMB pretreatment.

Next, based on previously confirmed culture conditions [8], after the addition of treated RS (5.5 g), *Phanerochaete chrysosporium* ATCC 32629 was cultured in 250 mL of optimized fungal medium, containing 1 % (*w*/*v*) glucose as an additional carbon source, for 12 days at 29 °C and 150 rpm. The spores of *P. chrysosporium* from potato dextrose agar after 10 days were suspended in 0.85 % (*w*/*v*) saline and subsequently counted using a Neubauer chamber. For biodegradation experiments, 30 mL of medium was added to 100-mL flasks, which was inoculated with a sufficient amount of suspension to obtain an initial concentration of 2.8×10^6 spores/mL. Cultures were incubated at 29 °C and 150 rpm for 80 h. At the large-scale stage (110 g RS biomass/5 L), the input concentration (i.e., 2 %) for the initial population of fungal cells used was maximal for the 100 mL stock solution with 1 % (*w*/*v*) glucose. No substrate was added to the control sample. In addition, to control unstable parameters (e.g., protein concentration, growth rate, and pH), statistical downstream concepts were followed via the Box-Behnken and Placket-Burman methodologies [8], and target maximization for the fungal medium via manganese peroxidase (MnP) was carried out in the closed WSMB process. In particular, the three core components for an optimized platform were determined as yeast extract, KH_2PO_4, and $CaCl_2$. Under the identified WSMB conditions, the extracellular levels of MnP was predicted to be approximately 2780 U/L. Its corresponding activity from actual experiments was in good agreement with the predicted value.

Biochemical Indices for Downstream Evaluation

In an open stage with a combination of either extracellular or intracellular cascades, the value of inhibitory compounds, especially acetic acid, hydroxymethylfurfural, and furfural, and the maximum industrial efficiencies, especially of simultaneous fermentability and biodegradable digestibility of the WSMB-pretreated RS, were checked following the biomass methods described by the National Renewable Energy Laboratory (http://www.nrel.gov/biomass/analytical_procedures.html). Particularly, hydrolytic efficiency (Eq. (1)) was determined by subjecting samples to 60 filter paper units (FPU) of cellulase (Celluclast 1.5 L, Sigma-Aldrich, St. Louis, MO, USA) and 30 cellobiase units (CBU) of β-glucosidase (Novozyme 188, Sigma-Aldrich) per gram of glucan at pH 4.8, 50 °C, and 150 rpm for 120 h. In addition, the fermentable yield (Eq. (2)), based on simultaneous saccharification and fermentation, was determined using the RS substrate with 3.1 % (*w*/*v*) glucan in 250 mL of medium and *Saccharomyces cerevisiae* D5A (ATCC 200062), 30 CBU of β-glucosidase, and 15 FPU of cellulase per gram of glucan at an initial pH of 5.0. All samples were cultured at 150 rpm and 38 °C for 144 h. Simultaneously, the significant change in major components, especially lignin, glucan, and xylan, of treated RS were analyzed on a dry weight basis.

$$\text{Hydrolytic yield (\%maximum)} = \frac{\text{g of glucose by HPLC}}{\text{g of glucan} \times 1.1} \times 100 \quad (1)$$

$$\text{Fermentation yield (\%maximum)} = \frac{\text{g of ethanol}}{\text{g of glucan} \times 1.1 \times 0.511} \times 100 \quad (2)$$

Based on broadly accepted protocols (Supporting Information), the extracellular activities of well-known target enzymes such as lignin peroxidase (LiP), MnP, xylanase, β-glucosidase, and cellulose dehydrogenase (CDH) that are involved in lignocellulose biocascades were predicted during the WSMB process. All experiments were conducted in triplicate.

After the WSMB program, the microstructural property of the RS substrates was observed using a Hitachi S-4700 microscope (Tokyo, Japan). Moreover, the functional spectra of samples were determined with a Bruker D5005 diffractometer (Karlsruhe, Germany) to understand the crystallinity change of WSMB-pretreated RS. The conserved signals were checked in triplicate using the previously reported θ–2θ system [9].

Proteomic Pool Analysis for Upstream Evaluation

Under different biodegradation conditions, regardless of whether a water soaking-based system is used, the complementary relationship between biocascade targets and percent theoretical yields was predicted by an analysis of proteomic expression. After preprocessing, i.e., protein isolation (Supporting Information) of *P. chrysosporium* pellets (after 12 days), the conserved mapping of the fungal proteome was carried out using a two-dimensional electrophoresis (2-DE) system to identify the quantitative patterns of changing targets following exposure to WSMB-treated RS. Further details regarding the 2-DE procedure are provided in the Supporting Information. After the electrophoresis, all spots exhibiting altered induction levels were systematically identified by either peptide mass fingerprinting or tandem mass spectrometry-based sequencing, based on the upstream information from public databases. Further details are provided in the Supporting Information. After six biological replicates of the biodegradation cultures, the statistical significance of all samples was calculated via both SAS ver. 9.2 (SAS Institute, Cary, NC, USA) and SigmaStat ver. 3.5 program (Systat Software, San Jose, CA, USA).

Results and Discussion

Bioconversion Yields of the WSMB System

In order to evaluate the relative industrial digestibility of WSMB treatment, the biodegraded RS was simultaneously hydrolyzed by the addition of both cellulase and β-glucosidase. The proactive index of the theoretically maximal glucose was 65.0 % (after stationary stage) from treated RS with biodegradation periods of 12 days (Table 1). Remarkably, the actual hydrolysis yield of biodegraded RS was a similar 64.9 % (after 120 h; [8]). The yield from the WSMB program, which is based on released monomeric sugars, was not higher than those of agricultural biomass deconstructed using physicochemical pretreatment processes (over 70 % based on mass balance) [10]. In particular, the fermentation productivity (approximately 0.52 g/L/h) of chemical-induced approaches, especially the ammonia-based platform [11], is greater than the productivity suggested by the WSMB (0.25–0.34 g/L/h). On the other hand, this biosystem is relatively superior to the others, especially the biological (23–45 % based on long-term cultivation) and alkaline (58–91 %) processes in terms of the economic feasibility [12–16]. Furthermore, the fermentable level (0.02–0.03 g ethanol/g renewable biomass) in unsystemized fungal processes was obtained after 120 h of bioconversion [17, 18], which was not more than the WSMB level (approximately 0.10 g ethanol/g substrate after 96 h).

Table 1 Downstream process index for scale-up in advanced WSMB process

Type	Initial substrate (dry wt. basis)	Sugar[b] (g/5 L)	Core parameters for industrial evaluation			
			Relative crystallinity/CrI[c]	Fermentability[d]	Biodegradability[e]	
					Biodegradation for 24 h	Biodegradation for 96 h
WSMB	120.0 g RS	<2.0	~62.7/~40.5	≤62.8 % (11.9 ± 0.2 g ethanol)	≤50.2 % (19.2 ± 0.4 g glucose)	≤65.0 % (24.8 ± 0.5 g glucose)
Untreated	120.0 g RS	Not detected	~56.4/~22.8	≤30.3 % (5.7 ± 0.1 g ethanol)	≤9.7 % (3.7 ± 0.1 g glucose)	≤27.5 % (10.5 ± 0.2 g ethanol)
PC[a]	120.0 g RS	Not detected	~56.2/~22.4	≤30.8 % (5.8 ± 0.1 g ethanol)	≤9.6 % (3.7 ± 0.1 g glucose)	≤28.6 % (10.9 ± 0.2 g ethanol)

[a] Positive control; RS biomass with mineral water-soaking pretreatment

[b] Free glucose (*w*/*v*) from biodegradable biomass during the water-soaking pretreatment

[c] Relative crystallinity $= \frac{\text{Crystalline intensity}}{\text{Crystalline intensity}+\text{Amorphous intensity}} \times 100$ and $\text{CrI} = 1-\frac{\text{Amorphous intensity}}{\text{Crystalline intensity}} \times 100$

[d] The yield of theoretical maximum ethanol based on the SSF after 96 h

[e] The yield of theoretical maximum glucose based on the WSMB after 12 days

Potential Changes in Microfibril Structures by a Closed WSMB System Without the Supply of External Substrates

When compared to the smooth base of untreated polymeric RS biomass, WSMB-pretreated surfaces were regularly degraded as a form of unwound fibers (Fig. 1). These data suggest that the extracellular change in crystalline fibrils can be proactively accelerated by inducible depolymerization by peroxidative enzymes (Fig. 2 and Tables 2 and 3) at all locations, water molecules, and reactive oxygen species, owing to soaking-based preprocess. Unlike the well-known diameter (below 10 nm) [19] of a single fibril, especially from vascular plants, the multilayered aggregate of biodegradable microfibrils was broadly found as uniform patterns in the range 2–10 μm (Fig. 1b). Interestingly, when compared to conventional chemical programs for dissolving the amorphous materials, especially based on dilute acid (approximately 9 μm) [20], the predominant difference in the morphological change in the twisted structures was hard to distinguish by WSMB. In particular, the active permeation of water molecules may have accelerated direct swelling by a simultaneous osmotic system [21] to a secondary or primary layer composed of biopolymeric modules. If water-soaking pretreatment helps to loosen the polysaccharide or lignin wall, then the extracellular peroxidative enzymes (Table 3) have more open space to contribute extensively. This means that the dynamic aggregative patterns of cross-linked fibrils in the plant cell walls have a fundamental gap in both conservative indices (here CrI; Table 3) [9] and mechanical properties, e.g., thermal expansion coefficient, Young's modulus, and reinforcing efficiency [22–24]. It is highly probable that the putative characteristics of fibril aggregates can be generated proactively by environmental damages, such as substrate modification, accelerating biochemical attacks, and oxidative stress.

The significant change in total mass of the internal components in bioprocessed RS after water-soaking was negligible to within an error range (Table 4). On the other hand, the core components (i.e., lignin, cellulose, and hemicellulose) of WSMB-based RS caused predominant reductions in dry mass compared to those of the control.

Proteomic Evaluation of Advanced WSMB Biosystem: Nonspecific Networking and Signaling Defense

In metabolic bioconversion systems of biomass materials, the homeostatic symphony of intracellular signaling factors may be a foregone conclusion based on the

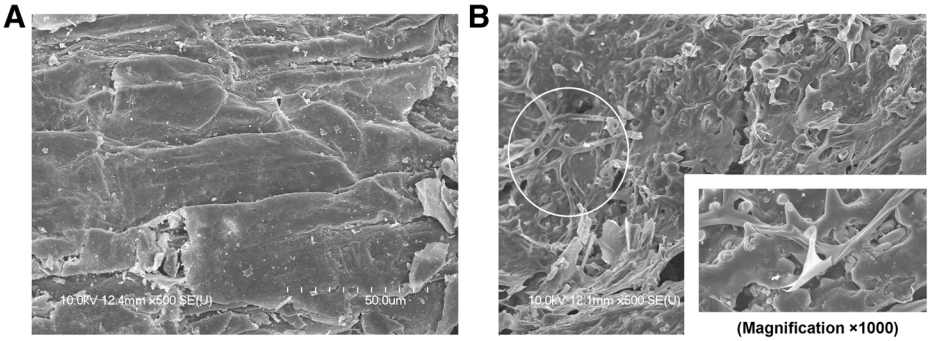

Fig. 1 Scanning electron microscopic image of depolymerized microfibrils from RS substrate that was biopretreated by advanced WSMB program. **a** Untreated RS. **b** RS biopretreated by optimal WSMB for 12 days

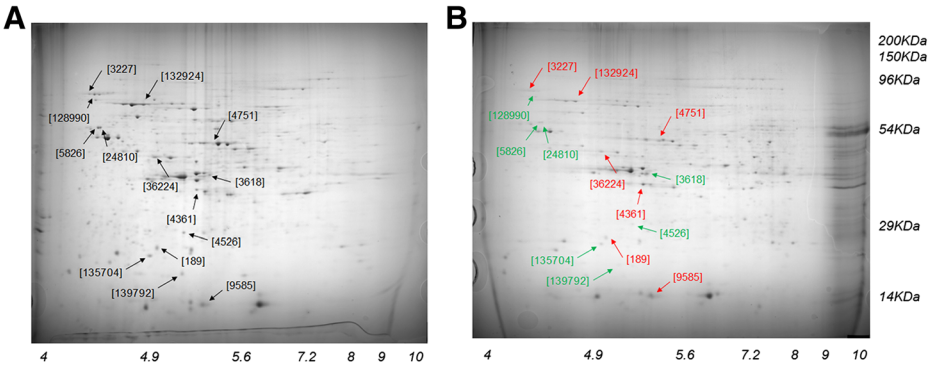

C

JGI ID	Putative function	*pI*/MW	Sequence	Cov. [a]
189	BTB/POZ domain	4.96/22.90	KELPGWDPDLFCR	54
3227	Tyrosine protein kinase	4.50/85.53	RNTFLR	86
4361	Cellulose-binding region	5.32/35.84	RLQAATQWLQQNNLK	47
4751	Ribose 5-phosphate isomerase	5.35/39.79	RVTVLDDGSQEVDLPGVGIR	31
9585	Intramembrane metalloprotease	5.29/12.11	RGGAEHLGWCMDSAWF	31
36224	Ureidoglycolate hydrolase	4.81/47.12	KLNMYPDGGIAR	67
132924	Heat shock protein 70	4.77/74.91	KFELSGIPPAPR	33
3618	Mitogen-activated protein kinase-interacting protein	5.24/38.46	RSFISPLLPGR	64
4526	Copper amine oxidase	5.17/26.22	RDWFDDDWGR	60
5826	Elongation factor 1	4.52/55.56	KLVPIGYGIR	60
24810	Serine/threonine protein kinase	4.54/55.34	KPSIEDQALTQLIDDAER	38
128990	Ubiquitin fusion degradation protein 2	4.53/85.20	RLGVFDR	57
135704	Predicted leucine zipper transcription factors, dopey family	4.94/20.87	RGSALNFLSR	50
139792	20S proteasome	5.15/17.07	KVEGTGR	57

Fig. 2 Differential proteomic display of conserved WSMB biocascade. Biodegradable organism (here *P. chrysosporium*) was continuously cultured for 12 days on **b** RS. The **a** control was grown without any biomass materials. Major 14 spots based on the two-dimensional gel electrophoresis represent metabolic signaling proteins with a statistical significance ($P < 0.05$ and $|\text{fold}| > 2$) compared with the corresponding targets in control. The expression levels are separately represented by either higher (*red*) or lower (*green*). **c** Identification of the selected intracellular proteins of *P. chrysosporium* multiplatform based on the US Department's Joint Genome Institute database. *Superscript letter a*, sequence coverage (%) in peptide mass fingerprinting

environmentally evolutionary process of survival [25, 26], suggesting that, remarkably, the effective yields of the bio-pretreatment platform may be involved in the proactive or interconnective regulation of upstream metabolic triggers, especially lignocellulolysis-induced signals.

To elucidate the conserved cellular biocascades of optimized WSMB by *P. chrysosporium*, the induction pattern of biodegradation-regulated targets was identified based on the mapping of the proteome profiles (Fig. 2). Interestingly, independent of either water-soaking preprocess or crystalline modification (e.g., CrI; Table 3), the general profile of major proteins involved in intracellular signaling and metabolic maintenance was significantly downregulated (Table 2), similar to that previously reported in a nonsoaking biosystem [8, 27]. Under harsh conditions with recalcitrant substrates, extravagant pathways, which involve the activation of lignocellulolytic targets, are not expected be initiated at the inactive cells, probably due to the optimized self-complementation mechanism (Tables 2 and 3) to achieve time/energy

Table 2 List of predominant proteome correlated with lignocellulolytic regulatory metabolism in open large-scale WSMB cascade

Target protein ID[a]	Putative biochemical function[a]	Change in expression[b]	Fold change value ($P < 0.05$) RS/control[c]
189	BTB/POZ domain	Upregulation	2.0
3227	Tyrosine protein kinase	Upregulation	2.6
4361	Cellulose-binding region	Upregulation	2.3
4751	Ribose 5-phosphate isomerase	Upregulation	4.7
9585	Intramembrane metalloprotease	Upregulation	2.2
36224	Ureidoglycolate hydrolase	Upregulation	2.3
132924	Heat shock protein 70	Upregulation	4.4
3618	Mitogen-activated protein kinase-interacting protein	Downregulation	0.28
4526	Copper amine oxidase	Downregulation	0.13
5826	Elongation factor 1	Downregulation	0.19
24810	Serine/threonine protein kinase	Downregulation	0.30
128990	Ubiquitin fusion degradation protein 2	Downregulation	0.27
135704	Predicted leucine zipper transcription factors, dopey family	Downregulation	0.43
139792	20S proteasome	Downregulation	0.18

[a] Based on the US Department's Joint Genome Institute upstream database

[b] Expression of RS compared to that of control (no substrate)

[c] Relative fold change ratio of the targets between RS and control

saving (Table 1). Therefore, the activation of a flow-dependent balance against undesirable external damages may not easily maintain more spontaneous biodegradation but can still be supported in the passive improvement of percent yields, due to the conditions of minimal growth during the long-term bioplatform and stress tolerance (Tables 1 and 2). In particular, the spontaneous limitation of protein kinases, especially mitogen-activated protein kinase-interacting protein and serine/threonine protein kinase (Table 2), in closed WSMB after 12 days may interrupt signal transduction for growth and the biodegrading cascade but can be accelerated by both structural deconstruction and morphological modification of amorphous or crystalline fibrils [28]. Additionally, the practical feedback for extracellular validation was obtained as significant structural indices of polysaccharide components (Tables 1 and 4). On the other hand, the overexpressed performance of some kinases, such as tyrosine protein kinase, is based on the stability of either a de novo managing system [29] or a cellular damage bioplatform [30] and can maintain metabolic balance over an entire process of closed WSMB (Table 2). Furthermore, in order to support the cellular differentiation based on the long-term cultivation bioprocess, the pentose phosphate pathway, e.g., ribose 5-phosphate isomerase, may be activated rather than lignocellulolytic cascades in spite of ligninolytic maximization. The low induction of transcription factors, especially elongation factor 1, was shown to offer a lethargic defense against programed cell damages during conserved endoplasmic stress [31]. Lastly, the proactive presence of heat shock protein 70 for the protein folding

Table 3 Extracellular potential of major lignocellulolytic enzymes in improved WSMB metabolism

Type	ROS[b] (mmol/L)	Actual activity of key targets (U/L)				
		Manganese peroxidase	Lignin peroxidase	Cellobiose dehydrogenase	β-Glucosidase	Hemicellulolytic xylanase
WSMB	<0.02	1100–1600	550–800	~90	~160	~475,000
Untreated	Not detected	Not detected	Not detected	Not detected	Not detected	Not detected
PC[a]	Not detected	Not detected	Not detected	Not detected	Not detected	Not detected

[a] Positive control; RS biomass with mineral water-soaking pretreatment

[b] Reactive oxygen species; especially H_2O_2

Table 4 Analysis of biorefinery-based compounds in advanced WSMB program

Type	Substrate (dry wt. basis)	Lignocellulosic hydrolysates[b] (*w*/*w*, %) (before/after)			Inhibitory byproducts		
		Lignin	Cellulose (g glucan)	Hemicellulose (g xylan)	Furfural[c] (*w*/*w*, %)	Hydroxymethylfurfural[c] (*w*/*w*, %)	Acetate (g/5 L)
WSMB	110.0 g RS	22.7/17.3	40.5/33.6	12.3/9.6	Not detected	Not detected	<0.5
Untreated	110.0 g RS	22.7/22.7	40.5/40.5	12.3/12.3	Not detected	Not detected	<0.2
PC[a]	110.0 g RS	22.7/22.7	40.5/40.5	12.3/12.3	Not detected	Not detected	<0.3

[a] Positive control; RS biomass with mineral water-soaking pretreatment

[b] Main biodegradable hydrolysates obtained from RS after the WSMB

[c] Confirmed as $\frac{\text{g of furfural of treated RS}}{\text{g of initial weight of RS}} \times 100$ and $\frac{\text{g of hydroxymethylfurfural of treated RS}}{\text{g of initial weight of RS}} \times 100$

mechanism shows that the WSMB bionetwork can universally protect the damaged cells from stress [32]. It also contributes to the development of stable biodegradation networks and reduces unneeded infrastructures such as the 20S proteasome and ubiquitin fusion degradation protein 2.

Multiple Target-Specific Deconstruction of Open Cellulosic Microfibrils

Based on WSMB proteome data (Fig. 2 and Table 2), the connective modules of both carbohydrate-active enzymes (CAZys; especially cellulose-binding region) and the ligninolytic degraders, ureidoglycolate hydrolase as a glyoxalate generator, as the hydrolysable triggers, were responsible for the optimized metabolic conversion of pre-processed RS into a fermentable carbon chain and ethanol. Remarkably, the expression level of CAZys, namely β-glucosidase, CDH, and hemicellulolytic xylanase, which are target factors for the practical downstream index, and peroxidative enzymes, including copper amine oxidase, in WSMB had a very low rate (fold <2) of intracellular activities in the context of cellulolytic mechanism, unlike previously identified microbial biosystems [26, 33, 34]. This difference is likely due to the platform being optimized for extracting cellulosic microfibers, which is based on the ligninolytic cascade via target optimization, especially by MnP. However, the extracellular bioplatform with conserved stability did not yet rule out the minor triggers, which draw the actual possibility on either process stability or recuperative strength (Table 3). Interestingly, the inevitable targets in the extracellular platform for maintaining lignocellulolytic biocascades can be spontaneously and simultaneously activated, regardless of the uniform exposure of nonamorphous fibers [8, 27]. The driving loss of three key components, as well as the rising trend of industrial yields, supported the powerful action of practical extracellular networks (Tables 1 and 4).

Based on the proteomic display, the presence of open twisted cellulosic microfibers (by direct WSMB) could give a greater depth to the substrate-specific response of the independent *P. chrysosporium* mechanism. In other words, a bypass of mainstream or a complementation of substream in the intracellular WSMB system is based on a matter of homeostatic equilibrium and signaling stability, rather than kaleidoscopic style of biodegradable substrates such as polymeric structures and components (Figs. 1 and 2 and Tables 1, 2, and 4).

Conclusions

Based on scale-up mass balance, the WSMB-pretreated RS showed significant increases in practical yields compared to the untreated RS after 12 days. Particularly, the systematic understanding of microfibril aggregates revealed that the physicochemical modifications in lignocellulosic surfaces are likely a leverage of the WSMB process. It is dominant in enhancing biological platform for fermentation stability but not in applying the industrial efficiency for downstream bioprocesses. Although the theoretical maximum of the bioplatform was lower than for biomass processed by conventional platforms, the metabolic inhibitors were rarely generated. Lastly, the conserved profiling of cellular proteins involved in lignocellulolytic biocascades during closed WSMB treatment could help the consolidated verification for interconnected probability and economic feasibility of either substrate-specific or nonspecific regulatory platforms.

Acknowledgments This work was supported by the by the Ministry of Education & Science Technology, Republic of Korea.

References

1. Chiaramonti, D., Prussi, M., Ferrero, S., Oriani, L., Ottonello, P., Torre, P., & Cherchi, F. (2012). Review of pretreatment processes for lignocellulosic ethanol production, and development of an innovative method. *Biomass and Bioenergy*, *46*, 25–35.
2. Sanderson, K. (2011). Lignocellulose: a chewy problem. *Nature*, *474*, S12–S14.
3. Menon, V., & Rao, M. (2012). Trends in bioconversion of lignocellulose: biofuels, platform chemicals & biorefinery concept. *Progress in Energy and Combustion Science*, *38*, 522–550.
4. Sims, R. E. H., Mabee, W., Saddler, J. N., & Taylor, M. (2010). An overview of second generation biofuel technologies. *Bioresource Technology*, *101*, 1570–1580.
5. Chaturvedi, V., & Verma, P. (2013). An overview of key pretreatment processes employed for bioconversion of lignocellulosic biomass into biofuels and value added products. *3 Biotech*, *3*, 415–431.
6. Fan, L. T., Gharpuray, M. M., & Lee, Y. H. (1987). *Cellulose hydrolysis*. Berlin:Springer-Verlag.
7. Park, S., Baker, J. O., Himmel, M. E., Parilla, P. A., & Johnson, D. K. (2010). Cellulose crystallinity index: measurement techniques and their impact on interpreting cellulase performance. *Biotechnology for Biofuels*, *3*, 10.
8. Bak, J. S., Ko, J. K., Choi, I. G., Park, Y. C., Seo, J. H., & Kim, K. H. (2009). Fungal pretreatment of lignocellulose by *Phanerochaete chrysosporium* to produce ethanol from rice straw. *Biotechnology and Bioengineering*, *104*, 471–482.
9. Bak, J. S., Ko, J. K., Han, Y. H., Lee, B. C., Choi, I. G., & Kim, K. H. (2009). Improved enzymatic hydrolysis yield of rice straw using electron beam irradiation pretreatment. *Bioresource Technology*, *100*, 1285–1290.
10. Agbor, V. B., Cicek, N., Sparling, R., Berlin, A., & Levin, D. B. (2011). Biomass pretreatment: fundamentals toward application. *Biotechnology Advances*, *29*, 675–685.
11. Ko, J. K., Bak, J. S., Jung, M. W., Lee, H. J., Choi, I. G., Kim, T. H., & Kim, K. H. (2009). Ethanol production from rice straw using optimized aqueous-ammonia soaking pretreatment and simultaneous saccharification and fermentation processes. *Bioresource Technology*, *100*, 4374–4380.
12. Potumarthi, R., Baadhe, R. R., Nayak, P., & Jetty, A. (2013). Simultaneous pretreatment and sacchariffication of rice husk by *Phanerochete chrysosporium* for improved production of reducing sugars. *Bioresource Technology*, *128*, 113–117.
13. Sharma, R., Palled, V., Sharma-Shivappa, R. R., & Osborne, J. (2012). Potential of potassium hydroxide pretreatment of switchgrass for fermentable sugar production. *Applied Biochemistry and Biotechnology*, *169*, 761–772.
14. Dias, A. A., Freitas, G. S., Marque, G. S. M., Sampaio, A., Fraga, I. S., Rodrigue, M. A. M., Evtuguin, D. V., & Bezerra, R. M. F. (2010). Enzymatic saccharification of biologically pre-treated wheat straw with white-rot fungi. *Bioresource Technology*, *101*, 6045–6050.
15. Zhao, Y., Wang, Y., Zhu, J. Y., Ragauskas, A., & Deng, Y. (2008). Enhanced enzymatic hydrolysis of spruce by alkaline pretreatment at low temperature. *Biotechnology and Bioengineering*, *99*, 1320–1328.
16. Kim, S., & Holtzapple, M. T. (2005). Lime pretreatment and enzymatic hydrolysis of corn stover. *Bioresource Technology*, *96*, 1994–2006.
17. Shi, J., Sharma-Shivappa, R. R., Chinn, M., & Howell, N. (2009). Effect of microbial pretreatment on enzymatic hydrolysis and fermentation of cotton stalks for ethanol production. *Biomass and Bioenergy*, *33*, 88–96.
18. Shrestha, P., Rasmussen, M., Khanal, S. K., Pometto 3rd, A. L., & van Leeuwen, J. H. (2008). Solid-substrate fermentation of corn fiber by *Phanerochaete chrysosporium* and subsequent fermentation of hydrolysate into ethanol. *Journal of Agricultural and Food Chemistry*, *56*, 3918–3924.
19. Somerville, C., Bauer, S., Brininstool, G., Facette, M., Hamann, T., Milne, J., Osborne, E., Paredez, A., Persson, S., Raab, T., Vorwerk, S., & Youngs, H. (2004). Toward a systems approach to understanding plant cell walls. *Science*, *306*, 2206–2211.
20. Nuruddin, M., Chowdhury, A., Haque, S. A., Rahman, M., Farhad, S. F., Sarwar Jahan, M., & Quaiyyum, A. (2011). Extraction and characterization of cellulose microfibrils from agricultural wastes in an integrated biorefinery initiative. *Cellulose Chemistry and Technology*, *45*, 347–354.
21. Szymanski, D. B., & Cosgrove, D. J. (2009). Dynamic coordination of cytoskeletal and cell wall systems during plant cell morphogenesis. *Current Biology*, *19*, R800–R811.
22. Zimmerman, T., Pohler, E., & Schwaller, P. (2005). Mechanical and morphological properties of cellulose fibril reinforced nanocomposites. *Advanced Engineering Materials*, *7*, 1156–1161.
23. Nishino, T., Matsuda, I., & Hirao, K. (2004). All-cellulose composite. *Macromolecules*, *37*, 7683–7687.
24. Sakurada, I., Nukushima, Y., & Ito, I. (1962). Experimental determination of the elastic modulus of crystalline regions oriented polymers. *Journal of Polymer Science*, *57*, 651–660.

25. Bak, J. S. (2015). Extracellular breakdown of lignocellulosic biomass by *Dichomitus squalens*: peroxidation-based platform and homeostatic regulation. *Biotechnology Letters*, *37*, 349–358.
26. Cullen, D., & Kersten, P. J. (2004). Enzymology and molecular biology of lignin degradation. In R. Brambl, & G. A. Marzluf (Eds.), *The mycota III: biochemistry and molecular biology*. Berlin: Springer-Verlag.
27. Bak, J. S. (2014). Process evaluation of electron beam irradiation-based biodegradation relevant to lignocellulose bioconversion. *SpringerPlus*, *3*, 487.
28. Yennawar, N. H., Li, L. C., Dudzinski, D. M., Tabuchi, A., & Cosgrove, D. J. (2006). Crystal structure and activities of EXPB1 (Zea m 1), a β-expansin and group-1 pollen allergen from maize. *Proceedings of the National Academy of Sciences*, *103*, 14664–14671.
29. Robitaille, A. M., Christen, S., Shimobayashi, M., Cornu, M., Fava, L. L., Moes, S., Prescianotto-Baschong, C., Sauer, U., Jenoe, P., & Hall, M. N. (2013). Quantitative phosphoproteomics reveal mTORC1 activates de novo pyrimidine synthesis. *Science*, *339*, 1320–1323.
30. Ongkeko, W. M., Altuna, X., Weisman, R. A., & Wang-Rodriguez, J. (2005). Expression of protein tyrosine kinases in head and neck squamous cell carcinomas. *American Journal of Clinical Pathology*, *124*, 71–76.
31. Talapatra, S., Wagner, J. D. O., & Thompson, C. B. (2002). Elongation factor-1 alpha is a selective regulator of growth factor withdrawal and ER stress-induced apoptosis. *Cell Death and Differentiation*, *9*, 856–861.
32. Morano, K. A. (2007). New tricks for an old dog: the evolving world of Hsp70. *Annals of the New York Academy of Sciences*, *1113*, 1–14.
33. Fernandez-Fueyo, E., Ruiz-Dueñas, F. J., Ferreira, P., Floudas, D., Hibbett, D. S., Canessa, P., Larrondo, L. F., James, T. Y., Seelenfreund, D., Lobos, S., Polanco, R., Tello, M., Honda, Y., Watanabe, T., Watanabe, T., Ryu, J. S., Kubicek, C. P., Schmoll, M., Gaskell, J., Hammel, K. E., St John, F. J., Vanden Wymelenberg, A., Sabat, G., Splinter BonDurant, S., Syed, K., Yadav, J. S., Doddapaneni, H., Subramanian, V., Lavín, J. L., Oguiza, J. A., Perez, G., Pisabarro, A. G., Ramirez, L., Santoyo, F., Master, E., Coutinho, P. M., Henrissat, B., Lombard, V., Magnuson, J. K., Kües, U., Hori, C., Igarashi, K., Samejima, M., Held, B. W., Barry, K. W., LaButti, K. M., Lapidus, A., Lindquist, E. A., Lucas, S. M., Riley, R., Salamov, A. A., Hoffmeister, D., Schwenk, D., Hadar, Y., Yarden, O., de Vries, R. P., Wiebenga, A., Stenlid, J., Eastwood, D., Grigoriev, I. V., Berka, R. M., Blanchette, R. A., Kersten, P., Martinez, A. T., Vicuna, R., & Cullen, D. (2012). Comparative genomics of *Ceriporiopsis subvermispora* and *Phanerochaete chrysosporium* provide insight into selective ligninolysis. *Proceedings of the National Academy of Sciences*, *109*, 5458–5463.
34. Vanden Wymelenberg, A., Gaskell, J., Mozuch, M., Sabat, G., Ralph, J., Skyba, O., Mansfield, S. D., Blanchette, R. A., Martinez, D., Grigoriev, I., Kersten, P. J., & Cullen, D. (2010). Comparative transcriptome and secretome analysis of wood decay fungi *Postia placenta* and *Phanerochaete chrysosporium*. *Applied and Environmental Microbiology*, *76*, 3599–3610.